AGU ADVANCING EARTH AND SPACE SCIENCE

Geophysical Research Letters

RESEARCH LETTER
10.1029/2020GL091683

Hygroscopicity of Organic Aerosols Linked to Formation Mechanisms

Jieyao Liu[1], Fang Zhang[1], Weiqi Xu[2], Yele Sun[2], Lu Chen[1], Shangze Li[1], Jingye Ren[1], Bo Hu[2], Hao Wu[1], and Renyi Zhang[3]

[1]College of Global Change and Earth System Science, Beijing Normal University, Beijing, China, [2]State Key Laboratory of Atmospheric Boundary Layer Physics and Atmospheric Chemistry, Institute of Atmospheric Physics, Chinese Academy of Sciences, Beijing, China, [3]Departments of Atmospheric Sciences and Chemistry, Texas A&M University, College Station, TX, USA

Key Points:

- Remarkably-enhanced water uptake capacity of organic aerosol (OA) occurs on nucleation days
- A correlation between the hygroscopicity and oxidation state of OA is presented on new particle formation (NPF) days, and the correlation is absent on non-NPF days
- The photooxidation of volatile organic compounds to produce organic acids may dominate on NPF days, and the aqueous oligomerization might occur on non-NPF days

Supporting Information:

- Supporting Information S1

Correspondence to:

F. Zhang, Y. Sun and R. Zhang
fang.zhang@bnu.edu.cn;
sunyele@mail.iap.ac.cn;
renyi-zhang@tamu.edu

Citation:

Liu, J., Zhang, F., Xu, W., Sun, Y., Chen, L., Li, S., et al. (2021). Hygroscopicity of organic aerosols linked to formation mechanisms. *Geophysical Research Letters*, *48*, e2020GL091683. https://doi.org/10.1029/2020GL091683

Received 18 NOV 2020
Accepted 18 JAN 2021

Abstract Organic aerosols (OAs) account for a large fraction of tropospheric fine particulate matter, but the hygroscopicity of OA is poorly understood. Here, we show remarkably-enhanced water uptake capacity of OA due to formation of highly-oxidized oxygenated OA on new particle formation (NPF) events in Beijing. While non-nucleation processes also produce oxidized OA, their hygroscopicity exhibits little enhancement. As a result, a correlation between the hygroscopicity and oxidation state is absent for OA on non-NPF days. Further analysis reveals that the highly-oxidized oxygenated OA is 2.5 and 5-fold as hygroscopic as the oxidized primary OA and less-oxidized oxygenated OA, respectively. Our results suggest that nucleation-initiated photooxidation of volatile organic compounds to produce water-soluble organic acids may dominate on NPF days, and the aqueous oligomerization to yield less water-soluble products might occur on non-NPF days.

Plain Language Summary While organic aerosols (OAs) account for a large proportion of tropospheric fine particles, the water uptake capacity of OA is poorly understood. Here, we show distinct effects of different atmospheric processes on its hygroscopicity in polluted urban atmosphere. Remarkably-enhanced hygroscopicity is identified for OA formed from nucleation. Our results reveal that it is critical to account for the formation mechanisms in evaluating the impacts of OA on air quality and climate.

1. Introduction

The water uptake capacity of atmospheric aerosol particles impacts air quality and climate, by affecting the radiative forcing, visibility, and the ability to serve as cloud condensation nuclei (CCN; Hudson & Clarke, 1992; Qi et al., 2018). Organic compounds account for a large fraction (20% ~ 90%) of the total fine aerosol mass in the troposphere, but the water uptake capacity of organic aerosol (OA) is poorly known because of the presence of diverse organic species (Zhang et al., 2015). Some field studies estimated the water uptake capacity of OA using overall hygroscopicity of particles obtained from cloud condensation nuclei counter measurements and chemical composition based on κ-Köhler theory (Petters & Kreidenweis, 2007), showing that the hygroscopicity parameter (κ) of OA varies considerably from 0.03 to 0.3 because of the presence of different OA constituents (Chang et al., 2010; Deng et al., 2018; Mei et al., 2013). The hygroscopicity of OA varies largely depending on the chemical composition, types and emissions of gas precursors under different environmental conditions (Fan et al., 2020; Zhang et al., 2015). While OA with a higher degree of oxidation (e.g., highly-oxidized oxygenated OA) is typically hygroscopic (Qiu et al., 2020), there is large uncertainty about the hygroscopicity of OA with a lower degree of oxidation (e.g., less-oxidized oxygenated OA). Specifically, Xiao et al. (2011) found that 61% of the less-oxidized oxygenated OA in Guangzhou, China, is water-soluble, while Timonen et al. (2013) estimated that only 14% of less-oxidized oxygenated OA is water-soluble in Helsinki, Finland, using a similar method. The water solubility of primary sources of OA, such as the biomass burning and coal combustion OA, or aqueous-oxygenated OA, were investigated in urban Beijing (Hu et al., 2020; Qiu et al., 2019). However, a more quantitative investigation of the OA from different sources has been lacking.

OAs are produced both from primary emissions (e.g., primary OA or POA) and secondary formation (e.g., secondary OA or SOA). There exist two distinct growth mechanisms for OA formation, that is,

condensation/partitioning of low-to-intermediate products from volatile organic compounds (VOCs) photooxidation (Shrivastava et al., 2017) and aqueous processes including hydration, oligomerization, and acid-catalyzed reactions (Gomez et al., 2015; Xu et al., 2014; Zhang et al., 2015; Zhao et al., 2006). Laboratory experimental studies revealed that photooxidation products of VOCs enhances the particles hygroscopicity in varying degrees depending on the VOC types (e.g., Khalizov et al., 2013; Qiu et al., 2012; Guo et al., 2016), but oligomerization from aqueous reactions decreases the hygroscopicity (Xu et al., 2014). The studies suggest that, while photooxidation and oligomerization both increase the oxidation degree (i.e., an increasing O:C ratio), the two processes may lead to distinct hygroscopicity of OA. In addition, acid-base reactions, such as those between organic acids and amines, also enhance hygroscopicity (Gomez-Hernandez et al., 2016). In the atmosphere, VOCs oxidation from natural and anthropogenic sources leads to distinct product distributions (Zhang et al., 2015), and hygroscopicity of the products with multifunctional groups (i.e., with the carboxylic and hydroxyl functionalities, or glyoxal and methylglyoxal) are expected to be variable. For example, previous field study suggested that a decrease in hygroscopicity of OA due to the formation of biogenic SOA (formed from photooxidation of biogenic VOCs) during new particle formation (NPF) in forest region (Deng et al., 2018); Several other observations in urban atmosphere showed an enhanced aerosols water uptake capacity and CCN activity correlates with NPF events (Lance et al., 2013; Wu et al., 2016), but these studies discussed only the particles overall hygroscopicity, have not focused on the OA hygroscopicity yet. Currently, there is still a lack of understanding of the water uptake capacity for OA from multiple anthropogenic sources in polluted urban atmosphere. The OA dominates ambient fine composition in Beijing, with a mass fraction of 40–51% (Guo et al., 2014; Sun et al., 2015; Wang et al., 2016), and the composition of aerosol is complex due to both primary sources and secondary gas-to-particle conversion (Guo et al., 2014; Li et al., 2020; Ren et al., 2018; Zhang et al., 2015, 2019, 2020). With the aim of obtaining insights of the links between hygroscopicity of OA and its growth mechanisms, in this study, we retrieve and characterize the hygroscopic parameter of OA (κ_{org}) by using field campaign observed data of hygroscopic growth factor and chemical composition in urban Beijing. We focus on contrasting the κ_{org} between NPF and non-NPF events respectively in order to understanding the effect of different formation processes on hygroscopicity of OA.

2. Field Measurements and Methods

Field measurements of aerosol physical and chemical properties were conducted at the Institute of Atmospheric Physics (IAP) of Beijing during summer 2017. The measurements at the sampling site represent of typical pollution conditions in urban Beijing (Sun et al., 2015). The sampling period covered May 19 to June 18, 2017. A Scanning Mobility Particle Sizer (SMPS) was used to measure particle number distribution in the size range of 10–600 nm. The SMPS consisted of a long differential mobility analyzer (DMA; model 3081A, TSI Inc.) and a condensation particle counter (CPC; model 3775, TSI Inc.). The Hygroscopic Tandem Differential Mobility Analyzer (HTDMA) system was used to measure the hygroscopic growth factor (Gf) of particle. The HTDMA used in this study has been described previously (Fan et al., 2020; Levy et al., 2013; Wang et al., 2017; Zhang et al., 2017). In this study, the selected dry diameters were 40, 80, 110, 150, and 200 nm, respectively. A Nafion humidifier was used to humidify the quasi monodisperse particles to the specified relative humidity (90% RH). RH calibration was performed periodically with ammonium sulfate to maintaining RH within 90% ± 0.5%. A method developed by Gysel et al. (2009) was used to retrieve the Gf probability density function (PDF).

Non-refractory size-resolved submicron aerosol composition of Non-Refractory particulate matter (NR-PM_1 with diameter < 1 μm), including organics (Org), sulfate (SO_4), nitrate (NO_3), ammonium (NH_4), and chloride (Chl), was measured with an Aerodyne high-resolution time-of-flight aerosol mass spectrometer (HR-ToF-AMS) (Xu et al., 2015). Positive matrix factorization (PMF) analysis was performed to separate organic aerosol factors quantitatively by grouping the mass spectrometry and temporal variation for the purpose of source apportionment (Xu et al., 2017; Zhang et al., 2011). The ratio of oxygen to carbon (O:C) was determined by using an elemental analysis approach (Aiken et al., 2007). A five-factor solution was selected, including three SOA factors namely highly-oxidized oxygenated OA, less-oxidized oxygenated OA, and oxidized POA and two POA factors from hydrocarbon-like and cooking OA. The oxidized POA factor is related to higher signals of CO_2^+ and its spectrum is dominated by $C_xH_y^+$, indicating this kind of SOA is from the direct oxidation of POA (Xu et al., 2019), so it is named as oxidized POA. More details about operation of

the HR-AMS and PMF analysis can be found in supporting information (SI: Methods). We combined the bulk mass fraction of black carbon (BC) particles measured by a 7-wavelength aethalometer (AE33, Magee Scientific Corp; Zhao et al., 2017) with size-resolved BC distribution measured by a single particle soot photometer (SP2) in Beijing to obtain the size-resolved volume fraction of BC (Liu et al., 2019).

In this study, we use size-resolved κ derived from measured Gf to calculate the size-resolved κ_{org} based on the mixing rule with the size-resolved aerosol chemical compositions measured by AMS (Petters & Kreidenweis, 2007). The detailed calculation methods are presented in the supporting information (SI: Methods). Because the inversion involves measurements from HTDMA and AMS, we conducted a total mass closure to compare the mass concentration of PM_1 measured by the two techniques, which are well consistent during the field campaign (Figure S1).

3. Results and Discussion

3.1. κ_{org} on NPF and non-NPF Days

NPF events, which are characterized by a distinct "banana" shape in the time series of particle number size distribution (PNSD), occur frequently during the campaign (Figure 1a and Figure S2). In this study, with criteria of that, a distinct new mode of particles appears in the PNSD and prevails for more than an hour showing continuous growth (Dal Maso et al., 2005), typical NPF events occurred on 10 days, accounting for approximately 42% days during the entire period. The κ_{org} between NPF and non-NPF days is contrasted to evaluate the effect of different particle formation processes on hygroscopicity of OA.

The averaged diurnal variations of the PNSD, κ_{org} of different particle size on NPF days and non-NPF days are shown in Figure 1a. The obvious banana-shaped profile occurred around noontime and early afternoon (9:00–17:00 Local Time; LT) and is indicative of NPF (Figure 1a). The mean κ_{org} increases significantly when NPF occurs, while there is no increase in κ_{org} around noontime on non-NPF days (Figure 1a), particularly for the 40 nm particles. Compared with non-NPF days, the κ_{org} for 40–200 nm are noticeably higher on NPF days, with the largest disparity for 40 nm particles (Figure 1b) that is closely related to NPF. This suggests that the nucleation generates more hygroscopic OA. As a result, the κ_{org} is relative independent on particle size on NPF days when the nucleation enhanced the κ_{org}. On non-NPF days, the κ_{org} shows increase with increase of particle size because the larger particles are generally internally mixed and more aged and hygroscopic (Chen et al., 2020; Zhang et al., 2014). The mean bulk κ_{org} is 0.19 ± 0.07 and 0.11 ± 0.07 on NPF and non-NPF days, respectively, corresponding to a remarkable increase of 73% in κ_{org} and 20% in the overall hygroscopicity, κ_{bulk} (Table S1). Figure 1b shows that the volume fractions of less-oxidized oxygenated OA, hydrocarbon-like OA, and cooking OA are similar between NPF days and non-NPF days, while the frequency distribution of volume fraction of highly-oxidized oxygenated OA exhibits a significant shift from left to right, showing an increase from 15%-25% on non-NPF days to 20%-35% on NPF days (Figure 1c), accompanying with a decrease of volume fraction of oxidized POA from non-NPF to NPF days. This indicates that the NPF yield more highly-oxidized oxygenated OA. The "banana" type of NPF typically occurs under clear conditions with strong ultraviolet radiation (UV) and low RH (Figure S3) conditions. The mass loadings of SOA on NPF days highly depends on O_x ($O_x = NO_2 + O_3$) (Figure 1d), a conserved tracer of photochemical processing (Herndon et al., 2008; Xu et al., 2017). While, on non-NPF days, it closely depends on RH (Figure 1d). Therefore, nucleation due to the photooxidation of VOCs and subsequent growth of the nucleated particles generates large amounts of more water-soluble organic components, such as organic acids (Guo et al., 2020; Qiu et al., 2012), likely explaining the enhanced water uptake capacity of OA. On the other hand, non-NPF events typically correspond to polluted conditions with low UV and high RH (Figure S3; Guo et al., 2020), and oligomerization via aqueous reactions likely represents a key pathway for OA growth (Gomez et al., 2015; Zhao et al., 2006). This provides an explanation for the less hygroscopicity of OA during non-NPF events since primary OA (i.e., POA, hydrocarbon-like OA, and cooking OA) likely experiences significant growth by aqueous reactions to form less water-soluble oligomers (Xu et al., 2014). Our results indicate that NPF in polluted urban atmosphere, which is primarily driven by photochemical oxidation of anthropogenic VOCs (Guo et al., 2020), generates more hygroscopic OA. Another earlier study showed a weakened hygroscopicity of OA during NPF in a forest region area, where the newly formed particles are mainly formed from biogenic SOA (Deng et al., 2018), implying plausible effects of different NPF sources on hygroscopicity of OA.

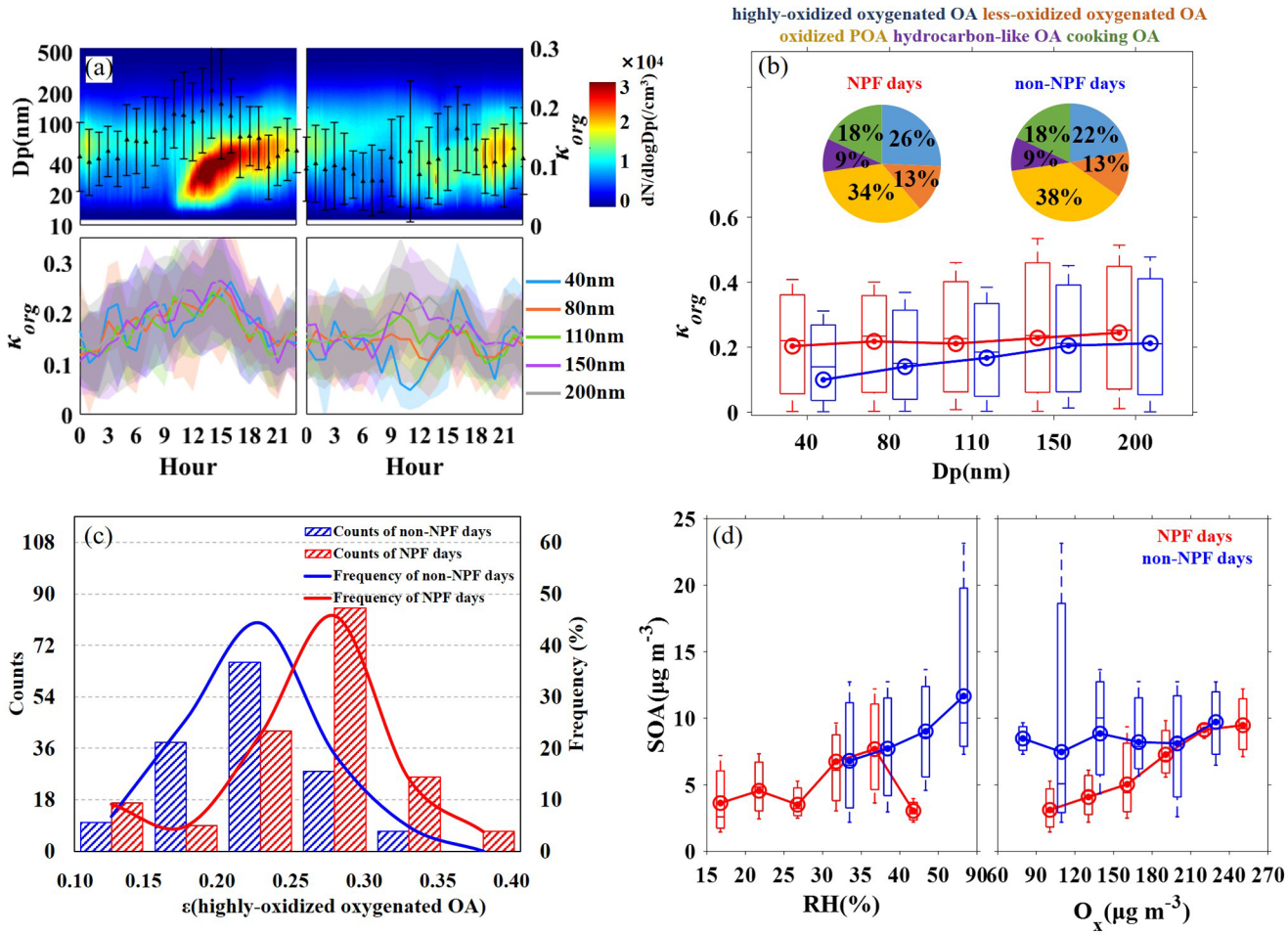

Figure 1. (a) Diurnal variations of PNSD and κ_{org} on NPF (left panels) and non-NPF days (right panels); The shade regions denote the error bars (±1σ). (b) The dependence of κ_{org} on D_p on NPF and non-NPF days during 9:00–15:00 LT. The pie charts embedded in the figure represent the mean volume fraction of five OA constituents during 9:00–15:00 LT. (c) The counts (left *y*-axis) and frequency (right *y*-axis) distribution of the volume fraction of highly oxidized oxygenated OA during 9:00–15:00 LT on NPF and non-NPF days. (d) Dependence of SOA mass concentration on RH and O_x on NPF and non-NPF days during 9:00–15:00 LT. The mean (circle), median (horizontal line), 25th and 75th percentiles (lower and upper box), and 5th and 95th percentiles (lower and upper whiskers) are presented in the figure. NPF, new particle formation; OA, organic aerosol; PNSD, particle number size distribution; RH, relative humidity; SOA, secondary organic aerosol.

3.2. Dependence of the κ_{org} on Volume Fraction of OA

The dependence of κ_{org} on the changes of the volume fraction of different kinds OA on NPF and non-NPF days is shown (Figure 2). The bulk κ_{org} increases monotonically (with a correlation coefficient, R^2, of >0.65 from different fits methods) from ~0.1 to ~0.22, when the volume fraction of highly oxidized oxygenated OA increases from ~18% to 27% (Figure 2a). On the other hand, an increase of κ_{org} with the volume fraction of less-oxidized oxygenated OA and oxidized POA are not apparent (Figure 2b and 2c). The remarkably larger κ_{org} always occurs during NPF events. In other words, OA from NPF exhibits the largest water uptake capacity, independent on changes in the fraction of the less-oxidized oxygenated OA and oxidized POA. Those results again indicate the critical role of nucleation process in enhancing the κ_{org}, while the aqueous oligomerization during non-NPF events yields less water-soluble products (e.g., oligomers; Xu et al., 2014). As a result, it shows that the hygroscopicity of highly-oxidized oxygenated OA is generally 2.5 and 5-folds of those of oxidized POA and less-oxidized oxygenated OA, respectively, illustrated by the slopes from a linear correlation analysis during the whole campaign (Figure 3). In addition, the increases of volume fraction of hydrocarbon-like OA and cooking OA result in decreasing κ_{org}. Note that, although both the cooking OA and hydrocarbon-like OA are thought to be nonhygroscopic (Petters & Kreidenweis, 2007), it shows that the

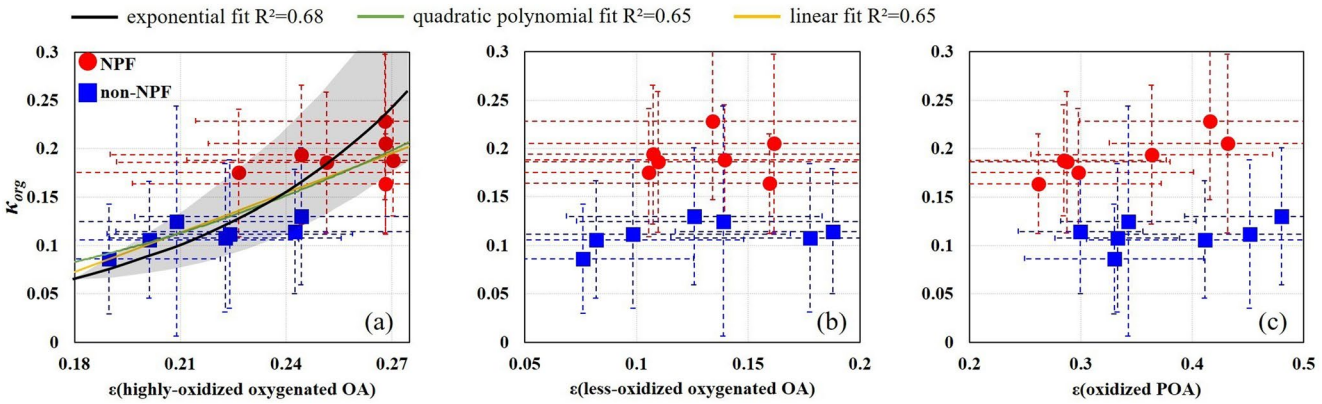

Figure 2. The dependence of κ_{org} on volume fraction of three OA types on NPF days (red dots) and non-NPF days (blue square) during 9:00–15:00 LT. (a) Highly oxidized oxygenated OA; (b) less-oxidized oxygenated OA; and (c) oxidized POA. Different fittings of κ_{org} and ε highly oxidized oxygenated OA are represented by lines of different colors: the exponential fit (black); quadratic polynomial fit (green); linear fit (orange). The gray shadow is an auxiliary display of exponential fitting. The error bars represent ±1σ. NPF, new particle formation; OA, organic aerosol; POA, primary organic aerosol.

former is less hydrophobic with less negative slope than that of the latter one, likely due to the lower ratio of O/C of hydrocarbon-like OA in Beijing than that of cooking OA (Sun et al., 2016).

3.3. Dependence of κ_{org} on f_{44} and O:C

To evaluate the oxidation degree on hygroscopicity, we assessed the dependence of changes of κ_{org} on the variations of f_{44} and O:C, along with comparison with previous studies (Figure 4). Figure 4a and 4b show that there exists little correlation of κ_{org} with f_{44} and O:C, indicating that both parameters alone cannot represent or parameterize the hygroscopicity of OA. The weak dependence of hygroscopicity of OA on the oxidation degree is attributable to the complex formation and composition of OA in this polluted urban area, considering the two growth mechanisms by photooxidation and oligomerization as well as their effects

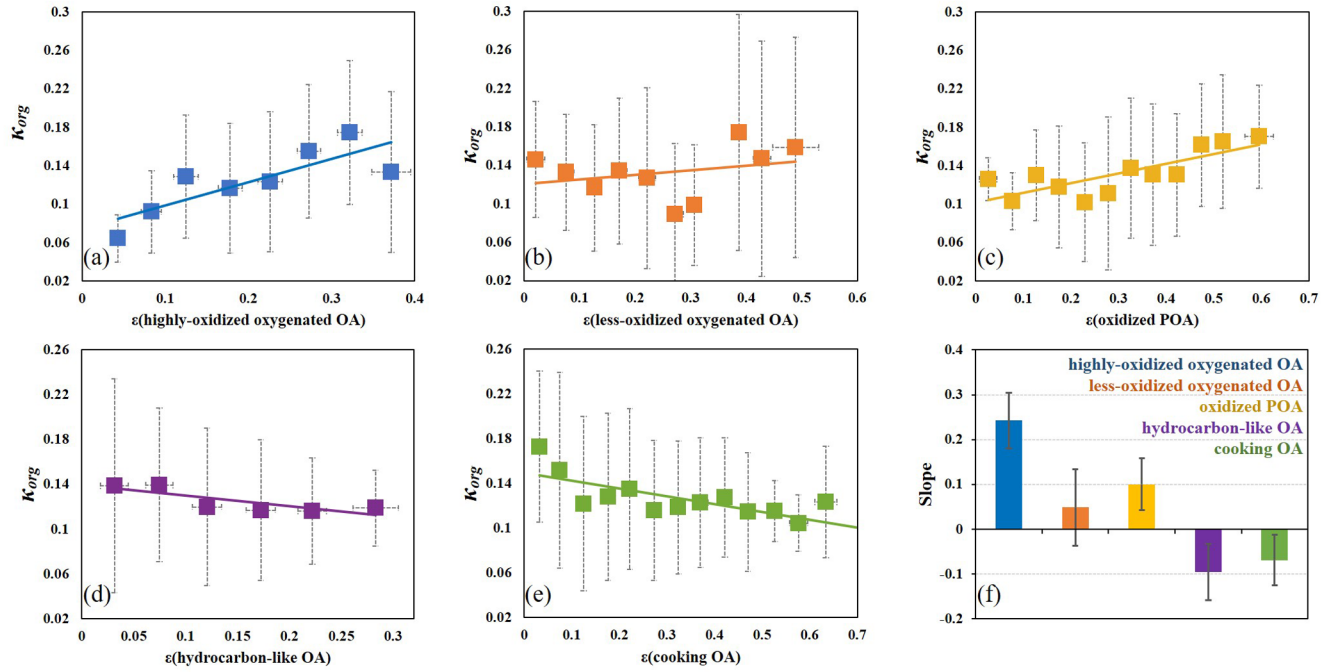

Figure 3. The dependence of κ_{org} on volume fraction of the five organic components ((a)–(e)) and the contribution (denoted by the slopes of the linear fit of κ_{org} vs. volume fraction of the five organics) of each component to κ_{org} (f). The error bars represent ±1σ.

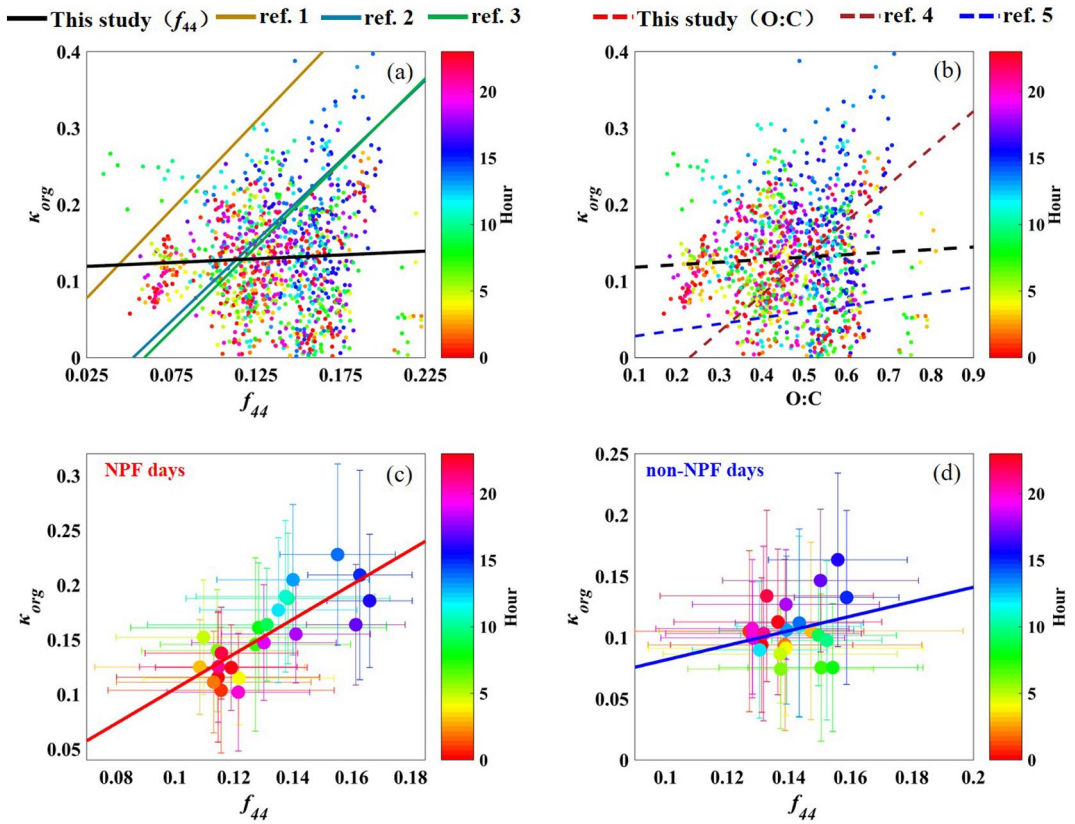

Figure 4. (a) The κ_{org} versus f_{44}. The dots with different color are f_{44} correspond to observed time of the day during the campaign as shown by the color bar. (b) The κ_{org} versus atomic O:C ratios. The dots with different color are atomic O:C ratios correspond to observed time of the day during the campaign as shown by the color bar. Also shown for comparison are literature results: ref. 1: Riau and Central Kalimantan, Indonesia (J. Chen et al., 2017); ref. 2: Sacramento, USA (Mei et al., 2013); ref. 3: Jungfraujoch and Mexico (Duplissy et al., 2011); ref. 4: Kyoto, Japan (Deng et al., 2018); ref. 5: Beijing (Wu et al., 2016). ref. 1–ref. 3: κ_{org} versus f_{44}. ref. 4 and ref. 5: κ_{org} versus O:C ratio. (c) The linear fitting of hourly averaged κ_{org} and f_{44} on NPF days; (d) The linear fitting of hourly averaged κ_{org} and f_{44} on non-NPF days. The error bars represent $\pm 1\sigma$.

on the oxidation state and hygroscopicity. A higher f_{44} occurs more frequently during daytime (around 10:00–15:00) on NPF days, when an improved correlation ($\kappa_{org} = 1.59 \times f_{44} - 0.05$, $R^2 = 0.61$) is obtained from the hourly mean κ_{org} as a function of the f_{44} values (Figure 4c). No apparent improved correlation is obtained when we link the κ_{org} to the fCO_2^+ ($\kappa_{org} = 1.50 \times fCO_2^+ - 0.03$, $R^2 = 0.57$; Figure S4) instead of f_{44} on NPF days due to that the CO_2^+ ion contributes about ~90–95% to f_{44}. Also, the correlation between κ_{org} and other AMS tracer ions fraction ($C_2H_3O^+$, CHO^+, $C_3H_5O^+$) is absent (Figure S4). This further demonstrated that these tracer ions are not sufficient to parameterize the κ_{org} since the OA molecular information is missing from the AMS measurements. The evidence of a larger f_{44} corresponding to higher κ_{org} during daytime on NPF days also implies that more hygroscopic OA is mainly produced from strong photochemical oxidation during nucleation process. On the other hand, the non-NPF processes result in higher f_{44} but less hygroscopic OA, and thus a poor correlation (Figure 4d), consistent with oligomerization with an increasing oxidation but lower κ_{org}. Our result contrasts with those previously observed at remote forest sites by Deng et al. (2018) and Chen et al. (2017); both studies showed apparent dependence of κ_{org} on f_{44}, when OA is formed from biogenic precursors. At a relative clean site, Zhang et al. (2014; 2016) also found that the higher f_{44} corresponds to high hygroscopicity and CCN activity. The distinct chemical composition, formation mechanisms, and the types of VOCs jointly regulate the variation in water uptake capacity of OA with the oxidation degree or f_{44} values (Timonen et al., 2013; Xu et al., 2014, 2017). Therefore, this study provides further evidence that the oxidation state alone is insufficient to characterize hygroscopicity, the molecular information of OA and unique formation mechanisms should be considered.

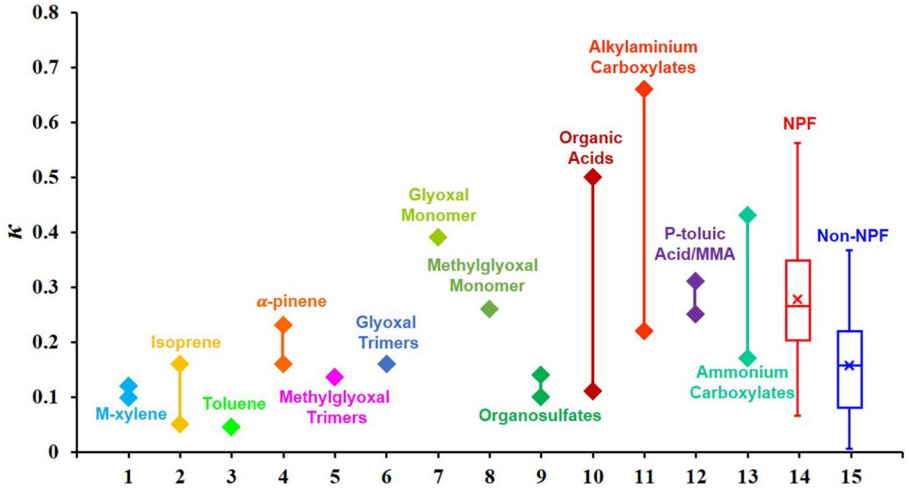

Figure 5. The κ values for different kinds of organics reported in literatures (1. Guo et al., 2016; 2. Khalizov et al., 2013; 3. Qiu et al., 2012; 4. Ma et al., 2013; 5-8. Xu et al., 2014; 9. Estillore et al., 2016; 10. Petters and Kreindenweis, 2007; Kumar et al., 2009; 11, 12. Gomez-Hernandez et al., 2016; 13. Dinar et al., 2008) and that measured on NPF and non-NPF days. NPF, new particle formation.

3.4. Comparison of the Field Observed Hygroscopicity of OA with that of Different Kinds of Organics

To further obtain insights on the formation of organic aerosols and the link to hygroscopicity of OA, we compare the field observed hygroscopicity of secondary formed OA (e.g., highly or less-oxidized oxygenated OA) with that of different kinds of organics (Figure 5). The hygroscopic parameter of these SOA (κ_{SOA}) is calculated by assuming the POA (e.g., cooking or hydrocarbon-like OA) is hydrophobic with κ value of 0. On NPF days, these secondary formed OA is very hygroscopic, with mean κ_{SOA} of 0.28 ± 0.12, and the value can be as high as 0.56. The results show that the water uptake capacity of the OA on NPF days is similar to that of organic acids, alkylaminium carboxylates or organic ammonia (Figure 5), which are reported more water soluble with κ of about 0.1–0.5 (Kumar et al., 2009; Petters & Kreidenweis, 2007), 0.2–0.66 (Gomez-Hernandez et al., 2016), and 0.17–0.43 (Dinar et al., 2008), respectively. This may indicate that the very hygroscopic OA, such as organic acids, carboxylic organic amine and ammonia organic salts may be largely formed during the nucleation and growth process on NPF days in polluted urban Beijing. On non-NPF days, the mean κ_{SOA} is 0.15 ± 0.09, with maximum value of 0.37, showing much weaker water uptake capacity than that of obtained during NPF days. The values on non-NPF days are closer to those of organic polymer (e.g., methylglyoxal trimer, glyoxal trimer dihydrate [GTD]; Xu et al., 2014) or organosulfates (e.g., benzyl sulfate; Estillore et al., 2016). Since the observed ratio of O:C is within the range of about 0.2–0.7 (Figure 4b), the organosulfates, which are generally with ratio of O:C of >1.0 (Altieri et al., 2009), should not be the primary products during our observed periods. In addition, these photochemical oxidation products of biogenic VOCs (e.g., isoprene, m-xylene; Guo et al., 2016; Khalizov et al., 2013; Ma et al., 2013), although which are with similar κ to that of our observation, are not expected to be dominant on non-NPF days due to low ambient concentrations in Beijing. While it is usually with high levels of anthropogenic VOCs (e.g., toluene, benzene) in urban atmosphere (Guo et al., 2020). In summary, the different formation mechanism of OA may explain the discrepancy of hygroscopicity of OA on NPF and non-NPF days. It is further demonstrated that the OA on NPF days may primarily formed by photooxidation, being more hygroscopic, while the non-NPF days the mechanism of oligomerization is dominant, yields less hygroscopic products. However, this needs to be fully clarified by the specific molecular information of OA in future field measurements.

4. Conclusions

While OA accounts for large proportion of ambient fine particles, the factors regulating the variations of its hygroscopicity remain unclear. Our simultaneous measurements of ambient fine particles chemical composition and hygroscopic growth factor during summer 2017 in Beijing reveal a remarkably-enhanced κ_{org} on

NPF days compared to non-NPF days. The mean κ_{org} of OA during NPF events is 0.19 ± 0.07, which is about 73% higher than that during non-NPF events. While non-nucleation processes (e.g., oxidized POA or oligomerization) also produce OA, their hygroscopicity exhibits little enhancement. A correlation between the hygroscopicity and oxidation state is absent for OA, indicating that the oxidation degree alone is insufficient to characterize hygroscopicity of OA in polluted urban atmosphere. Our results reveal that the measured distinct water uptake capacity of OA between NPF and non-NPF events is attributed to the different OA growth processes, that is, nucleation-initiated photochemical oxidation of VOCs to produce water-soluble products (e.g., organic acids) and aqueous oligomerization to yield less water-soluble products, respectively. The specific molecular information of OA warrants to be investigated combining other techniques (e.g., off-line ion chromatography) in future to provide direct evidence of our results inferred from the field measurements. Also, it is critical to account for the distinct OA growth mechanisms in atmospheric models for evaluation of their impacts on air quality and climate.

Data Availability Statement

All data used in the study are available on https://data.mendeley.com/datasets/3n72dcjdfv/1 or from the corresponding author upon request (fang.zhang@bnu.edu.cn).

Acknowledgments
This work was supported by the National Natural Science Foundation of China (Grants 41675141, 41975174), the National Basic Research Program of China (2017YFC1501702). The authors declare no competing financial interest.

References

Aiken, A. C., DeCarlo, P. F., & Jimenez, J. L. (2007). Elemental analysis of organic species with electron ionization high-resolution mass spectrometry. *Analytical Chemistry*, *79*(21), 8350–8358. https://doi.org/10.1021/ac071150w

Altieri, K. E., Turpin, B. J., & Seitzinger, S. P. (2009). Oligomers, organosulfates, and nitrooxy organosulfates in rainwater identified by ultra-high resolution electrospray ionization FT-ICR mass spectrometry. *Atmospheric Chemistry and Physics*, *9*(7), 2533–2542. https://doi.org/10.5194/acp-9-2533-2009

Chang, R. Y.-W., Slowik, J. G., Shantz, N. C., Vlasenko, A., Liggio, J., Sjostedt, S. J., et al. (2010). The hygroscopicity parameter (κ) of ambient organic aerosol at a field site subject to biogenic and anthropogenic influences: Relationship to degree of aerosol oxidation. *Atmospheric Chemistry and Physics*, *10*(11), 5047–5064. https://doi.org/10.5194/acp-10-5047-2010

Chen, J., Budisulistiorini, S. H., Itoh, M., Lee, W.-C., Miyakawa, T., Komazaki, Y., et al. (2017). Water uptake by fresh Indonesian peat burning particles is limited by water-soluble organic matter. *Atmospheric Chemistry and Physics*, *17*(18), 11591–11604. https://doi.org/10.5194/acp-17-11591-2017

Chen, L., Zhang, F., Yan, P., Wang, X., Sun, L., Li, Y., et al. (2020). The large proportion of black carbon (BC)-containing aerosols in the urban atmosphere. *Environmental Pollution*, *263*(2020), 114507,1–114507,11. https://doi.org/10.1016/j.envpol.2020.114507

Dal Maso, M., Kulmala, M., Riipinen, I., Wagner, R., Hussein, T., Aalto, P. P., & Lehtinen, K. E. J. (2005). Formation and growth of fresh atmospheric aerosols: Eight years of aerosol size distribution data from SMEAR II, Hyytiälä, Finland. *Boreal Environment Research*, *10*(5), 323–336.

Deng, Y., Kagami, S., Ogawa, S., Kawana, K., Nakayama, T., Kubodera, R., et al. (2018). Hygroscopicity of organic aerosols and their contributions to CCN concentrations over a midlatitude forest in Japan. *Journal of Geophysical Research: Atmosphere*, *123*(17), 9703–9723. https://doi.org/10.1029/2017JD027292

Dinar, E., Anttila, T., & Rudich, Y. (2008). CCN activity and hygroscopic growth of organic aerosols following reactive uptake of ammonia. *Environmental Science & Technology*, *42*(3), 793–799. https://doi.org/10.1021/es071874p

Duplissy, J., DeCarlo, P. F., Dommen, J., Alfarra, M. R., Metzger, A., Barmpadimos, I., et al. (2011). Relating hygroscopicity and composition of organic aerosol particulate matter. *Atmospheric Chemistry and Physics*, *11*(3), 1155–1165. https://doi.org/10.5194/acp-11-1155-2011

Estillore, A. D., Hettiyadura, A. P. S., Qin, Z., Leckrone, E., Wombacher, B., Humphry, T., et al. (2016). Water uptake and hygroscopic growth of organosulfate aerosol. *Environmental Science & Technology*, *50*(8), 4259–4268. https://doi.org/10.1021/acs.est.5b05014

Fan, X., Liu, J., Zhang, F., Chen, L., Collins, D., Xu, W., et al. (2020). Contrasting size-resolved hygroscopicity of fine particles derived by HTDMA and HR-ToF-AMS measurements between summer and winter in Beijing: The impacts of aerosol aging and local emissions. *Atmospheric Chemistry and Physics*, *20*(2), 915–929. https://doi.org/10.5194/acp-20-915-2020

Gomez-Hernandez, M., McKeown, M., Secrest, J., Marrero-Ortiz, W., Lavi, A., Rudich,Y., et al. (2016). Hygroscopic characteristics of alkylaminium carboxylate aerosols. *Environmental Science & Technology, 50*(5), 2292–2300. https://doi.org/10.1021/acs.est.5b04691

Gomez, M. E., Lin, Y., Guo, S., & Zhang, R. (2015). Heterogeneous chemistry of glyoxal on acidic solutions. An oligomerization pathway for secondary organic aerosol formation. *The Journal of Physical Chemistry A*, *119*(19), 4457–4463. https://doi.org/10.1021/jp509916r

Guo, S., Hu, M., Lin, Y., Gomez-Hernandez, M., Zamora, M. L., Peng, J., & Zhang, R. (2016). OH-initiated oxidation of m-xylene on black carbon aging. *Environmental Science & Technology*, *50*(16), 8605–8612. https://doi.org/10.1021/acs.est.6b01272

Guo, S., Hu, M., Peng, J., Wu, Z., Zamora, M. L., Shang, D., et al. (2020). Remarkable nucleation and growth of ultrafine particles from vehicular exhaust. *Proceedings of the National Academy of Sciences of the United States of America*, *117*(7), 3427–3432. https://doi/10.1073/pnas.1916366117

Guo, S., Hu, M., Zamora, M. L., Peng, J., Shang, D., Zheng, J., et al. (2014). Elucidating severe urban haze formation in China. *Proceedings of the National Academy of Sciences of the United States of America*, *111*(49), 17373–17378. https://doi.org/10.1073/pnas.1419604111

Gysel, M., McFiggans, G. B., & Coe, H. (2009). Inversion of tandem differential mobility analyzer (TDMA) measurements. *Journal of Aerosol Science*, *40*(2), 134–151. https://doi.org/10.1016/j.jaerosci.2008.07.013

Herndon, S. C., Onasch, T. B., Wood, E. C., Kroll, J. H., Canagaratna, M. R., Jayne, J. T., et al. (2008). Correlation of secondary organic aerosol with odd oxygen in Mexico City. *Geophysical Research Letters*, *35*(15), 596–598. https://doi.org/10.1029/2008gl034058

Hudson, J. G., & Clarke, A. D. (1992). Aerosol and cloud condensation nuclei measurements in the Kuwait plume. *Journal of Geophysical Research*, *97*(D13), 14533–14536. https://doi.org/10.1029/92jd00800

Hu, R., Xu, Q., Wang, S., Hua, Y., Bhattarai, N., Jiang, J., & Hao, J. (2020). Chemical characteristics and sources of water-soluble organic aerosol in southwest suburb of Beijing. *Journal of Environmental Sciences*, *95*(2020), 99–110. https://doi.org/10.1016/j.jes.2020.04.004

Khalizov, A. F., Lin, Y., Qiu, C., Guo, S., Collins, D., & Zhang, R. (2013). The role of OH-initiated oxidation of isoprene in aging of combustion soot. *Environmental Science & Technology*, *47*(5), 2254–2263. https://doi.org/10.1021/es3045339

Kumar, P., Barrett, D. M., Delwiche, M. J., & Stroeve, P. (2009). Methods for pretreatment of lignocellulosic biomass for efficient hydrolysis and biofuel production. *Industrial & Engineering Chemistry Research*, *48*(8), 3713–3729. https://doi.org/10.1021/ie801542g

Lance, S., Raatikainen, T., Onasch, T. B., Worsnop, D. R., Yu, X.-Y., Alexander, M. L., et al. (2013). Aerosol mixing state, hygroscopic growth and cloud activation efficiency during MIRAGE 2006. *Atmospheric Chemistry and Physics*, *13*(9), 5049–5062. https://doi.org/10.5194/acp-13-5049-2013

Levy, M. E., Zhang, R., Khalizov, A. F., Zheng, J., Collins, D. R., Glen, C. R., et al. (2013). Measurements of submicron aerosols in Houston, Texas during the 2009 SHARP field campaign. *Journal of Geophysical Research*, *118*(18), 10518–10534. https://doi.org/10.1002/jgrd.50785

Liu, D., Joshi, R., Wang, J., Yu, C., Allan, J. D., Coe, H., et al. (2019). Contrasting physical properties of black carbon in urban Beijing between winter and summer. *Atmospheric Chemistry and Physics*, *19*(10), 6749–6769. https://doi.org/10.5194/acp-19-6749-2019

Li, S., Zhang, F., Jin, X., Sun, Y., Wu, H., Xie, C., et al. (2020). Characterizing the ratio of nitrate to sulfate in ambient fine particles of urban Beijing during 2018–2019. *Atmospheric Environment*, *237*(2020), 117662,1–117662,12. https://doi.org/10.1016/j.atmosenv.2020.117662

Ma, Y., Brooks, S. D., Vidaurre, G., Khalizov, A. F., Wang, L., & Zhang, R. (2013). Rapid modification of cloud-nucleating ability of aerosols by biogenic emissions. *Geophysical Research Letters*, *40*(23), 6293–6297. https://doi.org/10.1002/2013gl057895

Mei, F., Setyan, A., Zhang, Q., & Wang, J. (2013). CCN activity of organic aerosols observed downwind of urban emissions during CARES. *Atmospheric Chemistry and Physics*, *13*(24), 1215–12169. https://doi.org/10.5194/acp-13-12155-2013

Petters, M. D., & Kreidenweis, S. M. (2007). A single parameter representation of hygroscopic growth and cloud condensation nucleus activity. *Atmospheric Chemistry and Physics*, *7*(8), 1961–1971. https://doi.org/10.5194/acp-7-1961-2007

Qi, X. F., Sun, J. Y., Zhang, L., Shen, X. J., Zhang, X. Y., Zhang, Y. M., et al. (2018). Aerosol hygroscopicity during the haze red-alert period in December 2016 at a rural site of the North China plain. *Journal of Meteorological Research*, *32*(1), 38–48. https://doi.org/10.1007/s13351-018-7097-7

Qiu, C., Khalizov, A. F., & Zhang, R. (2012). Soot aging from OH-initiated oxidation of toluene. *Environmental Science & Technology*, *46*(17), 9464–9472. https://doi.org/10.1021/es301883y

Qiu, Y., Xie, Q., Wang, J., Xu, W., Li, L., Wang, Q., et al. (2019). Vertical characterization and source apportionment of water-soluble organic aerosol with high-resolution aerosol mass spectrometry in Beijing, China. *ACS Earth and Space Chemistry*, *3*(2), 273–284. https://doi.org/10.1021/acsearthspacechem.8b00155

Qiu, Y., Xu, W., Jia, L., He, Y., Fu, P., Zhang, Q., & Sun, Y. (2020). Molecular composition and sources of water-soluble organic aerosol in summer in Beijing. *Chemosphere*, *255*(2020), 126850,1–126850,12. https://doi.org/10.1016/j.chemosphere.2020.126850

Ren, J., Zhang, F., Wang, Y., Collins, D., Fan, X., Jin, X., et al. (2018). Using different assumptions of aerosol mixing state and chemical composition to predict CCN concentrations based on field measurements in urban Beijing. *Atmospheric Chemistry and Physics*, *18*(9), 6907–6921. https://doi.org/10.5194/acp-18-6907-2018

Shrivastava, M., Cappa, C. D., Fan, J., Goldstein, A. H., Guenther, A. B., Jimenez, J. L., et al. (2017). Recent advances in understanding secondary organic aerosol: Implications for global climate forcing. *Reviews of Geophysics*, *55*(2), 509–559. https://doi.org/10.1002/2016rg000540

Sun, Y., Du, W., Fu, P., Wang, Q., Li, J., Ge, X., et al. (2016). Primary and secondary aerosols in Beijing in winter: Sources, variations and processes. *Atmospheric Chemistry and Physics*, *16*(13), 8309–8329. https://doi.org/10.5194/acp-16-8309-2016

Sun, Y. L., Wang, Z. F., Du, W., Zhang, Q., Wang, Q. Q., Fu, P. Q., et al. (2015). Long-term real-time measurements of aerosol particle composition in Beijing, China: Seasonal variations, meteorological effects, and source analysis. *Atmospheric Chemistry and Physics*, *15*(17), 10149–10165. https://doi.org/10.5194/acpd-15-14549-2015

Timonen, H., Carbone, S., Aurela, M., Saarnio, K., Saarikoski, S., Ng, N. L., et al. (2013). Characteristics, sources and water solubility of ambient submicron organic aerosol in springtime in Helsinki, Finland. *Journal of Aerosol Science*, *56*(2013), 61–77. https://doi.org/10.1016/j.jaerosci.2012.06.005

Wang, G., Zhang, R., Gomez, M. E., Yang, L., Zamora, M. L., Hu, M., et al. (2016). Persistent sulfate formation from London Fog to Chinese Haze. *Proceedings of the National Academy of Sciences of the United States of America*, *113*(48), 13630–13635. https://doi.org/10.1073/pnas.1616540113

Wang, Y., Zhang, F., Li, Z., Tan, H., Xu, H., Ren, J., et al. (2017). Enhanced hydrophobicity and volatility of submicron aerosols under severe emission control conditions in Beijing. *Atmospheric Chemistry and Physics*, *17*(8), 5239–5251. https://doi.org/10.5194/acp-17-5239-2017

Wu, Z. J., Zheng, J., Shang, D. J., Du, Z. F., Wu, Y. S., Zeng, L. M., et al. (2016). Particle hygroscopicity and its link to chemical composition in the urban atmosphere of Beijing, China, during summertime. *Atmospheric Chemistry and Physics*, *16*(2), 1123–1138. https://doi.org/10.5194/acp-16-1123-2016

Xiao, R., Takegawa, N., Zheng, M., Kondo, Y., Miyazaki, Y., Miyakawa, T., et al. (2011). Characterization and source apportionment of submicron aerosol with aerosol mass spectrometer during the PRIDE-PRD 2006 campaign. *Atmospheric Chemistry and Physics*, *11*(1), 6911–6929. https://doi.org/10.5194/acp-11-6911-2011

Xu, W., Guo, S., Gomez-Hernandez, M., Zamora, M. L., Secrest, J., Marrero-Ortiz, W., et al. (2014). Cloud forming potential of oligomers relevant to secondary organic aerosols. *Geophysical Research Letters*, *41*(18), 6538–6545. https://doi.org/10.1002/2014gl061040

Xu, W. Q., Han, T. T., Du, W., Wang, Q. Q., Chen, C., Zhao, J., et al. (2017). Effects of aqueous-phase and photochemical processing on secondary organic aerosol formation and evolution in Beijing, China. *Environmental Science & Technology*, *51*(2), 762–770. https://doi.org/10.1021/acs.est.6b04498

Xu, W. Q., Sun, Y. L., Chen, C., Du, W., Han, T. T., Wang, Q. Q., et al. (2015). Aerosol composition, oxidation properties, and sources in Beijing: Results from the 2014 Asia-Pacific Economic Cooperation summit study. *Atmospheric Chemistry and Physics*, *15*(23), 13681–13698. https://doi.org/10.5194/acp-15-13681-2015

Xu, W., Sun, Y., Wang, Q., Zhao, J., Wang, J., Ge, X., et al. (2019). Changes in aerosol chemistry from 2014 to 2016 in winter in Beijing: Insights from high-resolution aerosol mass spectrometry. *Journal of Geophysical Research: Atmosphere*, *124*(2), 1132–1147. https://doi.org/10.1029/2018JD029245

Zhang, Q., Jimenez, J. L., Canagaratna, M. R., Ulbrich, I. M., Ng, N. L., Worsnop, D. R., & Sun, Y. L. (2011). Understanding atmospheric organic aerosols via factor analysis of aerosol mass spectrometry: A review. *Analytical and Bioanalytical Chemistry*, *401*(10), 3045–3067. https://doi.org/10.1007/s00216-011-5355-y

Zhang, F., Li, Y., Li, Z., Sun, L., Li, R., Zhao, C., et al. (2014). Aerosol hygroscopicity and cloud condensation nuclei activity during the AC-3Exp campaign: Implications for cloud condensation nuclei parameterization. *Atmospheric Chemistry and Physics*, *14*(24), 13423–13437. https://doi.org/10.5194/acp-14-13423-2014

Zhang, F., Li, Z., Li, Y., Sun, Y., Wang, Z., Li, P., et al. (2016). Impacts of organic aerosols and its oxidation level on CCN activity from measurement at a suburban site in China. *Atmospheric Chemistry and Physics*, *16*(8), 5413–5425. https://doi.org/10.5194/acp-16-5413-2016

Zhang, F., Ren, J., Fan, T., Chen, L., Xu, W., Sun, Y., et al. (2019). Significantly enhanced aerosol CCN activity and number concentrations by nucleation-initiated haze events: A case study in urban Beijing. *Journal of Geophysical Research: Atmosphere*, *124*(24), 14102–14113. https://doi.org/10.1029/2019JD031457

Zhang, R., Wang, G., Guo, S., Zamora, M. L., Ying, Q., Lin, Y., et al. (2015). Formation of urban fine particulate matter. *Chemical Reviews*, *115*(10), 3803–3855. https://doi.org/10.1021/acs.chemrev.5b00067

Zhang, F., Wang, Y., Peng, J., Chen, L., Sun, Y., Duan, L., et al. (2020). An unexpected catalyst dominates formation and radiative forcing of regional haze. *Proceedings of the National Academy of Sciences of the United States of America*, *117*(8), 3960–3966. https://doi.org/10.1073/pnas.1919343117

Zhang, F., Wang, Y., Peng, J., Ren, J., Zhang, R., Sun, Y., et al. (2017). Uncertainty in predicting CCN activity of aged and primary aerosols. *Journal of Geophysical Research: Atmosphere*, *122*(21), 11723–11736. https://doi.org/10.1002/2017jd027058

Zhao, J., Du, W., Zhang, Y., Wang, Q., Chen, C., Xu, W., et al. (2017). Insights into aerosol chemistry during the 2015 China Victory Day parade: Results from simultaneous measurements at ground level and 260 m in Beijing. *Atmospheric Chemistry and Physics*, *17*(4), 3215–3232. https://doi.org/10.5194/acp-17-3215-2017

Zhao, J., Levitt, N. P., Zhang, R., & Chen, J. (2006). Heterogeneous reactions of methylglyoxal in acidic media: Implications for secondary organic aerosol formation. *Environmental Science & Technology*, *40*(24), 7682–7687. https://doi.org/10.1021/es060610k